Design Overview and Performance Assessment of an Integrated Electro-Hydraulic Actuator (iEHA)

Seshan Calapatti Suresh [1], Hassan Assaf [1], Andrea Vacca [1], Howard Zhang [2]

1. Maha Fluid Power Research Centre, Purdue University, West Lafayette, IN, USA, scalapat@purdue.edu; Hassan.Assaf@cat.com; avacca@purdue.edu

2. Parker Hannifin Corporation, Macedonia, OH, USA, hzhang@parker.com

Abstract.

The recent electrification trend in mobile and aerospace applications is increasing interest in electro-hydraulic actuators (EHAs), which are essentially primary-controlled hydraulic cylinders with an electric prime mover. EHAs can achieve high energy efficiency, a desirable feature particularly for electrified vehicles. Moreover, when implemented in a self-contained arrangement, EHAs are particularly attractive, as they can serve as an alternative to electromechanical actuators, leveraging the typical advantages of hydraulics. However, existing EHA designs have a structure unsuitable for most mobile applications and do not fully leverage the benefits of component integration.

This paper proposes an innovative design for an integrated Electro-Hydraulic Actuator (iEHA) based on aggressive component integration. The electric prime mover and the hydraulic machine are encapsulated in the cylinder head, while the reservoir is integrated alongside the walls of the hydraulic cylinder. The internal flow connections allow the differential flow between the cylinder and reservoir to circulate through the electric machine, thereby enabling optimal heat removal from the electric machine. The paper details the design morphology, the hydraulic and cooling circuit, and the sizing of the internal components, with supporting simulation results.

Keywords. EHA, iEHA, Electrification, Thermal Analysis.

NOMENCLATURE

ϕ_A - Piston diameter [m]	ϕ_a - Rod diameter [m]
γ – Polytropic index of the charge gas for the Accumulator [-]	n_s - Rotary speed [rev/min]
A_A - Piston chamber area [m^2]	A_a - Rod chamber area [m^2]
A_{ce} – Accumulator heat exchange surface area [m^2]	dh – Accumulator heat exchange [W]
hgf – Thermal heat exchange between liquid and gas [W]	h_{conv} – Accumulator heat exchange coefficient [-]
k_{heat} – Accumulator heat exchange gain [-]	η_v - Volumetric efficiency [-]
n_s – Pump/ E-pump speed [RPS]	$n_{s,max}$ – Maximum pump/ E-pump speed [RPS]
p_0, p_1, p_2 – Accumulator pressures at corresponding pressures [bar]	P^P_{frict} – Frictional heat generated in pumping mode [kW]
P^M_{frict} – Frictional heat generated in motoring mode [kW]	Δp – Pressure drop across the high-pressure and low-pressure ports of the HM [bar]
Q_A – Piston chamber flowrate [m^3/s]	Q_a – Rod chamber flowrate [m^3/s]
Q_{in} – HM inlet flowrate [m^3/s]	Q_{out} – HM outlet flowrate [m^3/s]
S_l – Cylinder stroke [m]	τ – HM Torque [N/m]
T_g – Accumulator gas temperature [k].	T_l – Accumulator liquid temperature [k]
T_w – Accumulator wall temperature [k]	$tcgf$ – Thermal conductivity of the gas/.liquid [W/m k]
V_a – Rod chamber volume of the cylinder [m^3]	V_A – Piston chamber volume of the cylinder [m^3]
V_D - Pump/motor displacement [m^3 /rev]	ΔV – Change in volume of the Accumulator [Liters]
V_0, V_1, V_2 – Accumulator volume filled at 0%, 10%, 90% respectively [m^3]	$\dot{x}$ - Linear velocity [m/s]

Abbreviations

A1: Manifold - accumulator port 1	A2: Manifold - accumulator port 1
BPV: Bypass valve	C1: Manifold - cylinder piston chamber port
C2: Manifold - cylinder rod chamber port	CFD: Computational Fluid Dynamics
DRV: Dual Acting Pressure Relief Valve	DV1 and DV2: 2/2 direction control valves
EM: Electric Motor	EHA: Electro-Hydraulic Actuator

E-pump: Electro-hydraulic Pump	EHU: Electro Hydraulic Unit
iEHA: integrated Electro-Hydraulic Actuator	IGM: Internal Gear Machine
INV: Inverter	Pacc: Accumulator pressure
PMSM: Permanent Magnet Synchronous Motor	PRV: Pressure Relief Valve
Qacc: Accumulator flow	SHV: Shuttle Valve
THA: Thermo-Hydraulic Accumulator	THC: Thermo-Hydraulic Chamber
THFHE: Thermo-Hydraulic Flow with Heat Exchange	THPM: Thermo-Hydraulic Pump/ Motor

1. INTRODUCTION

Self-contained EHAs have been introduced decades ago for critical controls in aerospace applications, with clear reliability advantages over electromechanical actuators, EMAs [1]. Their usage can eliminate long hydraulic lines and reduce leakages. Most importantly, their high energy efficiency, comparable to that of electromechanical actuators [2], makes their use particularly attractive for electrified off-road vehicles. EHAs also consistently reduce the space-claims actuation system, even compared to EMAs [3]. In EHA, high efficiency is achieved through a throttle-less implementation of the primary control concept [4, 5], in which the electric machine and hydraulic machines (i.e., E-Pump) are regulated to precisely match the hydraulic cylinder's flow demand.

Additionally, several EHA concepts also enable energy recuperation during overrunning loads [6]. These positive, energetic features of EHAs have promoted the implementation of "distributed EHA", as conceptually represented in Fig. 1.1, in which all components of the EHA system are distributed across different locations within the machine. Examples include the systems by Qu et al. in [7, 8], which also demonstrate the flexibility of the distributed arrangement, enabling both open-circuit and closed-circuit primary-controlled configurations. However, these implementations do not exploit the potential advantages of component integration, such as reduced overall space requirements and leakage. Such benefits are clearly desirable for off-road machinery and clearly motivated efforts such as the implementation proposed by Pietrzyk et al. [9].

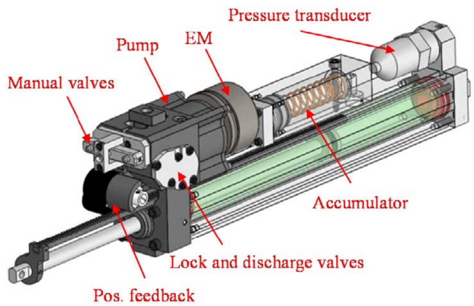

Figure 1.1. – Self-contained Electro Hydraulic Actuator designed by Altare et al. [10]

A clear challenge in deploying self-integrated EHAs in mobile applications, such as off-road machinery, is related to the design morphology. In fact, the typical design of a compact EHA resembles that of Fig. 1.1, where all the critical EHA elements are widely exposed to the surrounding environment. This arrangement is clearly unfavourable in harsh applications with a high risk of impact, such as construction equipment.

Integrated EHA typically require closed-circuit configurations of the hydraulic system, as in Fig. 1.2, that leverage pressurized reservoirs (usually low-pressure accumulators) for a flexible installation arrangement. In such a circuit, the cylinder extension and retraction always require flow corresponding to the displaced rod volume (usually referred to as differential flow). Creating control complexities and increasing the requirements on the hydraulic control system [11]. State-of-the-art EHAs do not leverage this differential flow for useful functions, such as heat dissipation, as in the proposed solution.

The present paper proposes a novel integrated design methodology for EHAs, particularly suitable for mobile applications. The study covers the design and the integration of the EHA, including component sizing and thermal behaviour analysis through simulations. The paper also discusses practical aspects of design integration and concludes with a summary of findings and conclusions.

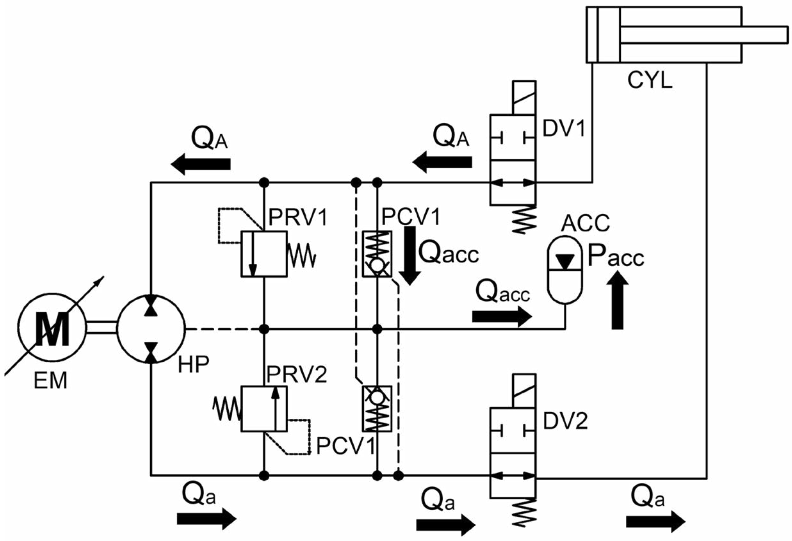

Figure 1.2. Closed-circuit EHA

The remainder of this paper is divided into the following sections. Section 2 presents the proposed electro-hydraulic actuator, including an overview and rationale, as well as its basic functioning, with isometric views and CAD details such as the cooling path. Section 3 describes the reference application and the choice of points for EHA functioning. Section 4 covers the basic component sizing, detailing the methods and final parameters for the electric machine, hydraulic machine, and Accumulator, along with the implications of the bypass valve. Section 5 provides practical information on design integration. Section 6 assesses the thermal behaviour through numerical simulations for the iEHA and cooling analysis for the electric motor. Finally, Section 7 concludes the paper by summarising the findings and conclusions.

2. INTEGRATED ELECTRO-HYDRAULIC ACTUATOR DESIGN

The principle of the proposed design is to maximize component integration, bringing the conventional architecture conceptually represented in Fig. 2.1(a) to a resulting architecture of Fig. 2.1(b). The Accumulator is concentric to the cylinder, and the E-pump is placed behind the cylinder on the same axis. Finally, the valve manifold is placed between the cylinder and the E-pump. The valve manifold not only serves as the point where all the valves are mounted but also as the part that provides hydraulic connections to all the components of the actuator. The proposed architecture leverages the known advantages for integrating electric and hydraulic machines (E-Pumps), in terms of magnet mass of the electric machine and overall dimension [12, 13,14], with additional advantages of integrating the pressurized reservoir within the hydraulic actuator. Additionally, an internal manifold valve integrates the hydraulic circuit, allowing for recirculation of the differential flow within the E-Pump. These features will be further detailed in the following subsections.

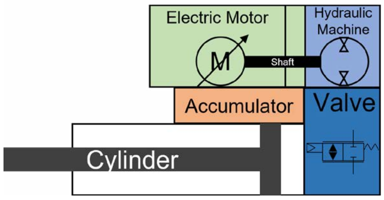

Figure 2.1(a). Traditional EHA design

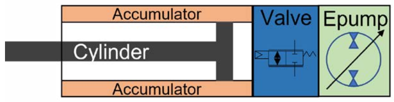

Figure 2.1(b). Proposed iEHA design

2.1. *Accumulator Design*

The low-pressure Accumulator is arranged concentric to the cylinder, similarly to a multi-chamber cylinder arrangement as commercialized by [15]. A ring-type piston is used to implement an original form of piston-type gas accumulator as shown in Fig. 2.2. Such a design not only reduces spatial requirement, but it is also adaptable to different piston strokes, as the volume requirement of the Accumulator linearly scales with the stroke length. The Accumulator uses the outer surface of the cylinder as one running surface, and a concentric cylinder running the entire length of the cylinder serves as the outer running surface for the Accumulator.

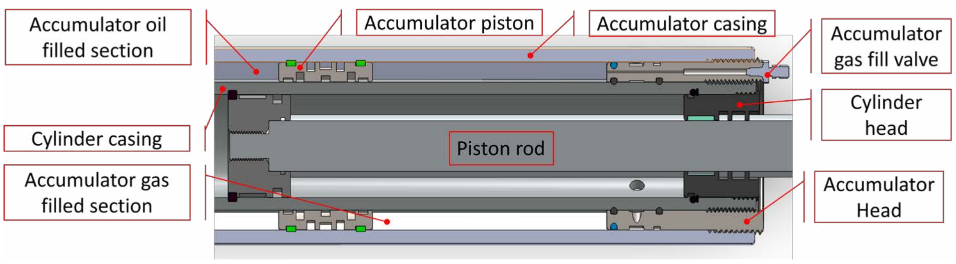

Figure 2.2: Accumulator design

2.2. *E-pump Design*

This section covers the design of the E-pump. The E-pump is designed based on the previous work by Pan and Zappaterra [13]. To enable energy recovery during assistive loading conditions, a four-quadrant hydraulic pump is required. Due to space constraints, a fixed-displacement pump is preferred, which also allows us to maintain a simple, compact design.

Considering the requirement of noise reduction, an internal gear pump is selected. And since internal gear pumps provide better filling and less noise [16] than external gear machines, a more compact design is possible. Moreover, using an internal gear pump offers a key advantage: the external gear can be directly driven, as illustrated in Fig. 2.3, resulting in a more compact E-pump design. In addition to its compactness, the internal gear pump can be designed so that the journal bearing supporting the external gear of the pump can also support the rotor of the electric motor [17]. Finally, the pump sizing is determined by the required flow rate derived from the cylinder specifications and the electric motor's maximum operating speed. Based on this, an internal gear machine with a 13-tooth pinion and a 19-tooth external gear was chosen.

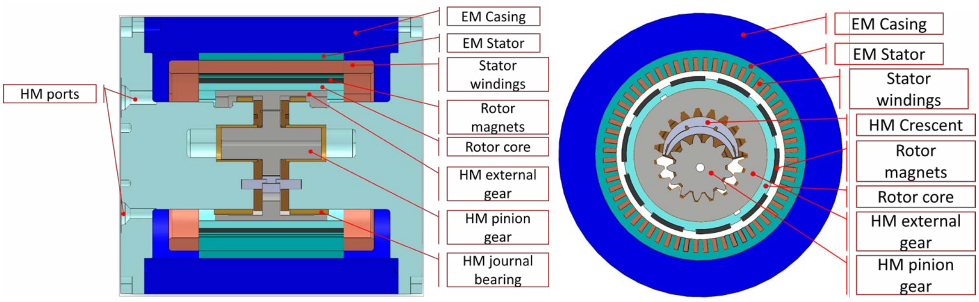

Figure 2.3(a). Radial cross-section Figure 2.3(b). Axial cross-section

Figure 2.3: E-pump design

A novel design feature of the E-pump design is using the differential flow to and from the Accumulator to cool the electric motor, as illustrated in Fig.2.5. The E-pump is designed so that the accumulator flow passes over the stator of the electric motor, thus cooling it. The flow path of the oil has been optimized using simulation to make sure that there are no hot spots in the stator. The heat energy transferred into the oil is later radiated into the atmosphere by the accumulator [18]. The E-pump design also discharges the drain flow into the differential flow.

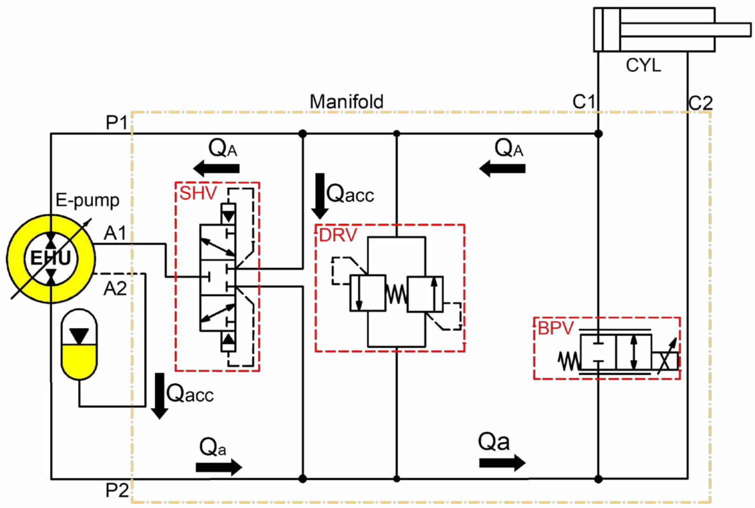

Figure 2.4 ISO schematic of the proposed EHA

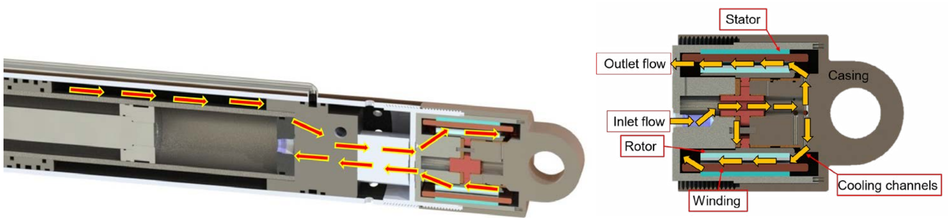

Figure 2.5. EHA Cooling flow path

2.3. Hydraulic circuit and valve manifold design

As illustrated in Fig. 2.4, the EHA was designed with three valves, of which one is a solenoid-operated proportional valve. This architecture represents the most minimalist implementation of a primary controlled circuit, where the low-pressure circuit is handled by an inverse shuttle valve (SHV) similar to that discussed in [19]. The circuit also includes a bypass valve (BPV) to improve control at low actuator velocities without running the E-pump at low RPMs. Moreover, as described in [20], the BPV also allows achieving high retraction velocities without increasing the E-pump's displacement, so that its displacement can be optimised to meet the maximum extension velocity requirement. To prevent any over-pressurisation events, a dual-acting version of an adjustable pressure relief valve (PRV) called the DRV was used. The DRV consists of 2 antiparallelly arranged pressure relief valves that are adjusted using a single screw. The final of the manifold design is shown in Fig. 2.6.

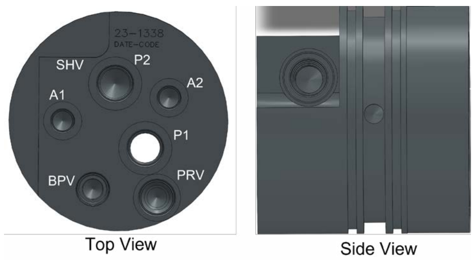

Figure 2.6: Manifold design

3. SIZING CONSIDERATIONS

The design sizing was based on considering the boom function of a mini excavator available in the market. The design data were obtained based on the cylinder size, velocity, and force required for the boom operation of a reference machine operated by an expert operator. Using this known data, a drive cycle was generated (shown in Fig. 3.3), and a basic assumption was made on the speed and torque requirements of the electric motor. Here, a design process, as shown in Fig. 3.1, was used to design and optimize the sizes of the electric motor, hydraulic pump, and manifold.

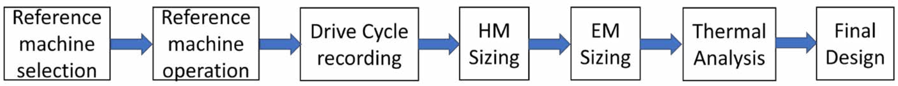

Figure 3.1: Designing procedure

After the initial design considerations were completed, particular attention to the packing of the integrated cylinder was taken into account. The valve locations impact how much they stick out for the manifold; this directly impacts the overall length of the cylinder. This is further complicated by the fact that the BPV, which requires exposure to air flow as it is solenoid-operated and requires cooling.

3.1. EHA operating points

As illustrated in Fig. 3.2, the design of the EHA components is based on a reference cycle to which the reference machine will be regularly subjected, as shown in Fig. 3.3. The electric motor power was selected based on the peak power in the reference drive cycle being run for a sustained period of time without leading to overheating.

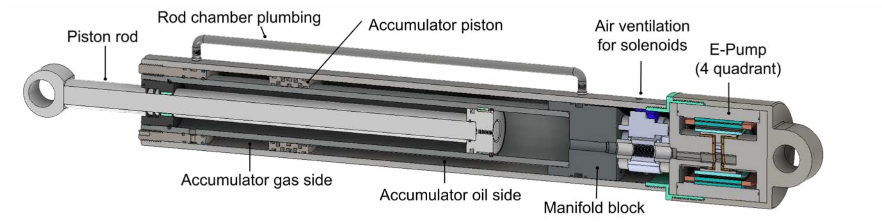

Figure 3.2 Design Overview

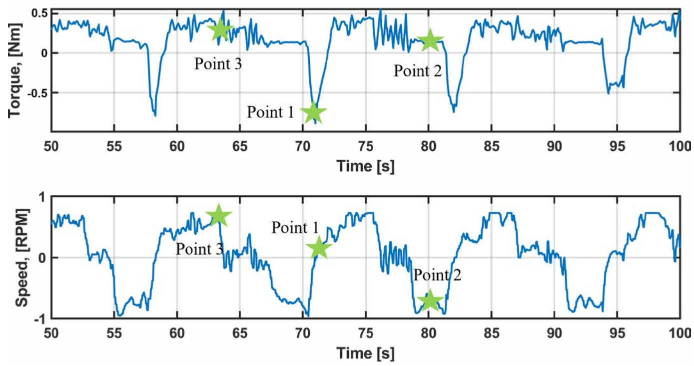

Figure 3.3 Operating points

4. BASIC COMPONENT SIZING

As detailed in Chapter 3, sizing begins with selecting a reference machine. Thus, the cylinder details are driven by the cylinder on the reference machine. The cylinder size then drives the volume of the Accumulator. The max velocity and the details of the cylinder drive the HM sizing. The HM size then determines the EM size. The sizing methodology used ensures that the EM's power rating accounts for all losses of earlier stages and can sustainably provide the power required for the reference drive cycle. Table 4.1 provides the normalized and relative cylinder details.

Parameters	*Symbol*	*Value*
Normalized Stroke length	S_l	1
Relative Piston Diameter	-	$S_l/7.1$
Relative Rod Diameter	-	$S_l/13.4$

Table 4.1 Normalized/ relative cylinder details

4.1. Electric motor sizing methodology & Final parameters

A Permanent Magnet Synchronous Motor (PMSM) was selected, as it offers very high power density. Furthermore, since the rotor of a PMSM comprises a set of magnets, the rotor core can be made hollow, allowing the hydraulic machine to nest inside the rotor.

The EM design was performed using GOSET software from Sudhoff [21]. This software is written in MATLAB and uses a multi-objective design approach to generate the EM design parameters based on the selected input parameters. The software generates a Pareto-optimal curve to select the optimal design. The software then uses the chosen design to develop the final EM design.

Parameters	***Symbol***	***Value***	***Units***
Nominal DC supply voltage	V_{DC}	800	[V]
Maximum motor speed	n_s	9500	[RPM]
Nominal motor torque	$\tau_{m,nom}$	25	[Nm]
Maximum motor torque	$\tau_{m,max}$	40	[Nm]

Table 4.2 EM input parameters

The input parameters are provided in Table 4.2. The input parameters are based on a drive cycle generated (Fig. 3 .3) using the methodology detailed earlier in this chapter, and on the choice of the battery and the inverter. Three points of interest from the drive cycle were selected based on the action being performed and the electric motor's instantaneous requirements. These 3 points cover the three most common modes of operation at regular loading conditions. Points 1 & 3 are a normal raising or quadrant one in Fig. 4.1. At point 1, the cylinder is starting to accelerate, and thus the EM speed is low, but the torque is at $\tau\ m$, max, But, at point 1, the cylinder is extending at high velocity and at no appreciable load. This requires a high EM speed and low torque. Point 2 is assistive retraction or quadrant four in Fig. 4.1. Here, the boom is lowering due to gravity, and thus energy recovery is possible. The final design parameters for the EM as detailed in Table 4.3

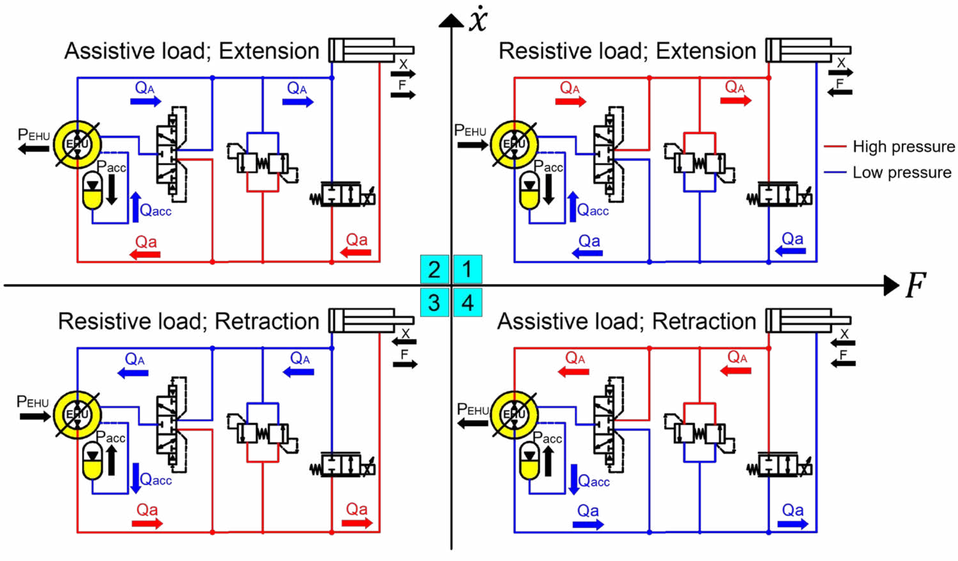

Figure 4.1 Operating modes of the EHA

Parameters	*Symbol*	*Value*	*Units*
Maximum motor speed	$n_{s,\,max}$	9500	[RPM]
Maximum motor torque	$\tau_{m,max}$	40	[Nm]

Table 4.3 Final EM parameters

4.2. Hydraulic machine sizing & Final parameter

The primary factor driving the design of the hydraulic machine is the maximum operating speed. The hydraulic machine is integrated into the rotor of the electric machine, resulting in a 1:1 gear ratio. Based on the conclusion from Zappaterra et al.[8] and Pietrzyk et al.[7]. An internal gear machine was determined to be suitable for this purpose.

The size of the hydraulic machine is determined by using Eqns.4.1 & 4.2. Based on the max velocity of the actuator during extension and the max rotational speed of the electric motor ($n_{s,\,max}$).

$$Q_A = \dot{x} \cdot A_A \tag{4.1}$$

$$V_D = \frac{Q_A \cdot \eta_v}{n_{s,max}} \tag{4.2}$$

In addition, the pump diameter is constrained by the electric motor's rotor diameter. This means that beyond a certain point, the length of the pump's gear set must increase to increase the displacement. Table 4.4 shows the final parameter for the hydraulic machine.

Parameters	*Symbol*	*Value*	*Units*
HM displacement	V_D	8	[cc]

Table 4.4. Final HM parameter

4.3. Accumulator sizing & Final parameters

Since a closed-circuit design was selected, an accumulator provides the differential flow of the cylinder. Hence, this is the primary driving factor for sizing the Accumulator. The cylinder's annular volume is derived from Eqn 4.3

$$V_a = A_a \cdot S_l \tag{4.3}$$

Based on the annular volume and the minimum and maximum accumulator pressures, the accumulator size is calculated using Eqns 4.4 & 4.5

$$\Delta V = V_0 \cdot p_0^{\frac{1}{\gamma}} \cdot \frac{p_2^{\frac{1}{\gamma}} - p_1^{\frac{1}{\gamma}}}{p_2^{\frac{1}{\gamma}} * p_1^{\frac{1}{\gamma}}} \tag{4.4}$$

$$V_0 = \frac{(\frac{p_2}{p_1})^{\frac{1}{\gamma}} \cdot \Delta V}{(\frac{p_0}{p_1})^{\frac{1}{\gamma}} \cdot \left[(\frac{p_2}{p_1})^{\frac{1}{\gamma}} - 1\right]} \tag{4.5}$$

The input parameters for the sizing of the accumulator are derived based on the cylinder details and are detailed in Table 4.5, and the final accumulator sizing is detailed in Table 4.6.

Parameters	*Symbol*	*Value*	*Units*
Charge gas	-	Nitrogen	[-]
Polytropic index	γ	1.4 @ 20°C	[-]
Precharge pressure	p_0	5.2	[bar]
Minimum working pressure	p_1	6.0	[bar]
Required volume	ΔV	3.44	[Liters]

Table 4.5 Accumulator input parameters

Parameters	*Symbol*	*Value*	*Units*
Accumulator volume	V_0	3.6	[Liters]
Maximum accumulator pressure	p_2	8.92	[bar]

Table 4.6 Accumulator final parameters

4.4. Bypass valve implications

The bypass valve is used in two scenarios. The primary use is to reduce the size of the hydraulic machine while achieving the same fast retraction velocity. The bypass valve is opened in quadrant 4 of Fig. 4.1(assistive retraction), which diverts some flow from the piston side chamber to the rod side of the cylinder. The secondary use is to allow high-velocity operation, especially when the hydraulic machine's speed falls below the minimum required to achieve this velocity.

5. DESIGN INTEGRATION

As mentioned, in the existing EHA designs, the components are externally connected to each other. This design aims to integrate all the components and place them on the same axis as the cylinder. For this reason, the majority of the components are cylindrical and are stacked. The Accumulator was designed to be concentric to the cylinder to increase the integration. The concentric cylinder would also allow the outer surface of the cylinder to be used as the inner running surface for the accumulator piston. Stacking/placing the manifold behind the cylinder will enable it to act as both the piston end cap of the cylinder and one of the end caps for the Accumulator, while providing fluid paths to both. The E-pump is placed/ stacked behind the manifold, and a connector connects the E-pump to the manifold. This connector also provides the space required for the valves. Since the outer running surface of the Accumulator is exposed to the environment, it can be used as a radiator for the heat generated. This eliminates the need for an additional external cooling system. Fig. 3.1 shows a near-complete design of the iEHA.

6. SIMULATION – THERMAL BEHAVIOUR & RESULTS

To access the thermal behaviour of the EHA, thermal simulations were conducted using two software packages. Simcenter's Amesim and Dassault Systèmes's SolidWorks were used to run thermal simulations of the complete EHA and the electric machine, respectively.

These simulations were performed using drive cycles generated to mimic the three loading points from Fig 3.3. The thermal simulation time period was set to a minimum of 9000 seconds for each drive cycle.

To ensure consistency between the two simulation methods. The boundary conditions (mainly the oil flowrate and oil pressure used to cool the E-Pump) and other parameters were obtained by first running the Amesim simulations using the generated drive cycles, capturing the data, and then using this data as inputs to the SolidWorks simulations.

6.1. Hydrothermal simulation using Amesim

As illustrated in Fig. 6.1, a thermal simulation model that considered both electrical and hydraulic characteristics was built and simulated, using the hydraulic equations from Chapter 4 for the hydraulic system. Further equations shown in this chapter were used to simulate thermal energy in electrical and hydraulic systems. Specifically, Eqs. 6.1 & 6.2 were used to build a discretized thermal model of the EM, accounting for energy loss due to electrical resistance and Eddy currents. The heat exchange between the oil and the EM is also simulated using a thermohydraulic flow model with heat transfer, and the contact areas were determined from the EM's 3D CAD. In addition, the accumulator oil flow path through the EM for cooling purposes was considered, along with the flow path lengths and diameters. Furthermore, the accumulator components used consider the design's features, and the design's dimensions are used to calculate the external surface area of the Accumulator in contact with the environment. A conservative wind speed and temperature were also considered.

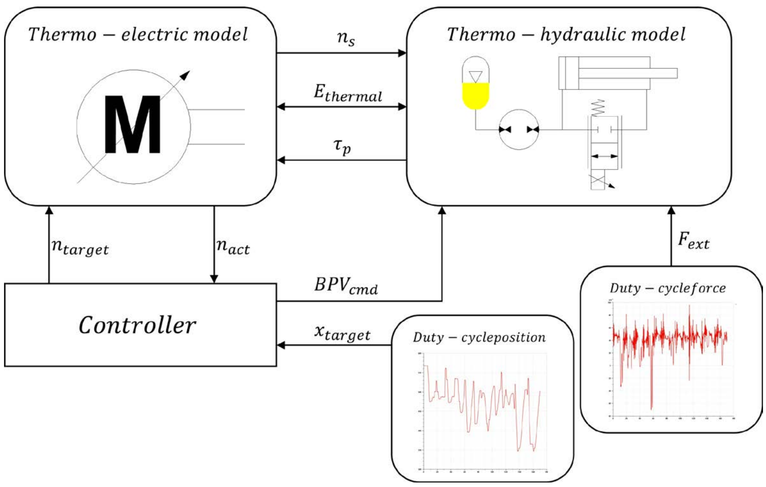

Figure 6.1 Simulation block diagram

$$dh_1 = \frac{t_2 - t_1}{TR} \tag{6.1}$$

$$\frac{dT}{dt} = \frac{\sum_{i=1}^{N} dh_i}{TC} \tag{6.2}$$

For the thermo-electric motor simulation, a lumped parameter RC model was built in Amesim. Fig. 6.2 illustrates an equivalent RC lumped parameter model. The thermal resistances (TR; illustrated by the black resistors in Fig. 6.2) and their heat flow rates are calculated using Eqn. 6.1. The thermal capacitances (TC) and the rate of change of temperature are computed using Eqn. 6.2. The EM lumped parameter model also accounts for the cooling oil flow and models the heat exchange using thermo-hydraulic flow with a heat exchange component in Amesin (THFHE; illustrated as red resistors in Fig. 6.2).

$$P_{frict}^{P} = (\tau \cdot \omega) - (Q_{in} \cdot \Delta p) \tag{6.3}$$

$$P_{frict}^{M} = (Q_{out} \cdot \Delta p) - (\tau \cdot \omega) \tag{6.4}$$

$$hgf = tcgf \cdot (T_g - T_l) \tag{6.5}$$

$$dh = k_{Heat} \cdot h_{conv} \cdot A_{ce} \cdot (T_l - T_w) \tag{6.6}$$

Furthermore, the thermo-hydraulic components we used for the hydraulic machine, cylinder and the Accumulator. As such, the friction in the pump/ motor is calculated using Eqn. 6.3 in pumping mode and Eqn. 6.4 in motoring mode. The heat exchange in the Accumulator is calculated using Eqn. 6.5. Finally, the heat exchange between the air and the Accumulator is calculated using Eqn. 6.6.

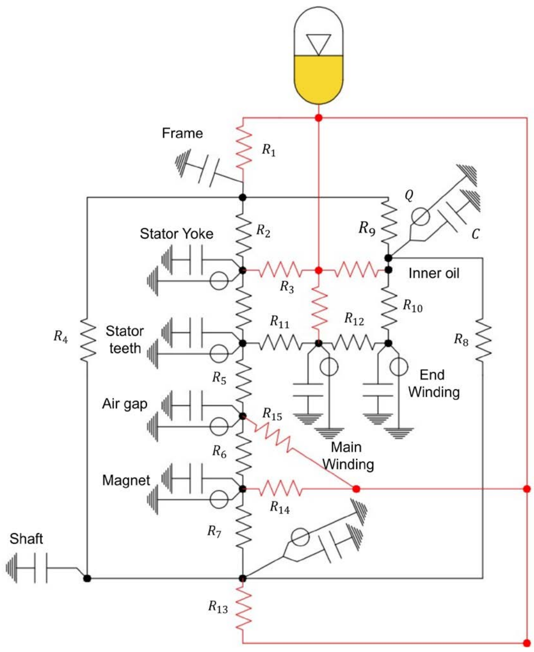

Figure 6.2 Equivalent EM lumped parameter model

6.2. *Thermal behaviour simulation using Amesim & SolidWorks*

In addition to the hydrothermal simulation in Amesim. A thermal simulation in SolidWorks was performed to verify the proper/ complete cooling of the EM. This simulation was performed on the standalone E-pump design with properties identical to those of the integrated E-pump design. The primary objective of simulating EM cooling using both a lumped-parameter Amesim model and a SolidWorks model was to verify that the lumped-parameter model accurately simulates the losses and temperatures of the EM. The secondary objective of the flow simulation was to verify the even cooling of the EM stator. The results and the subsequent comparison of the temperatures are shown in the Table. 6.1. The average temperature difference between the models was 1.6°C, and the maximum temperature difference was 4.0°C. Since the windings generate most of the heat and are the main priority, a total temperature reduction of 4.0°C (5.27%) is promising.

Location	***Amesim***	***SolidWorks***	***ΔT***
Winding	76.0	72.0	4.0
Stator	71.0	71.5	0.5
Magnet	54.0	54.0	0
Rotor core	53.6	54.2	0.6
Fluid at the outlet	54.1	57.0	2.9
Average deviation			1.6

Table 6.1 Temperature comparison

The secondary reason for this simulation was to ensure even & sufficient cooling of the EM. To access this, a further simulation was performed at multiple cylinder velocities to account for the varying cooling oil flow rates. As illustrated in Fig. 6.3, the fluid can evenly cool the EM, resulting in a maximum stator temperature of 76 °C. Fig. 6.4 also illustrates the temperature distribution in the EM. It can be observed that the maximum temperature deviation in the windings is 9.29°C.

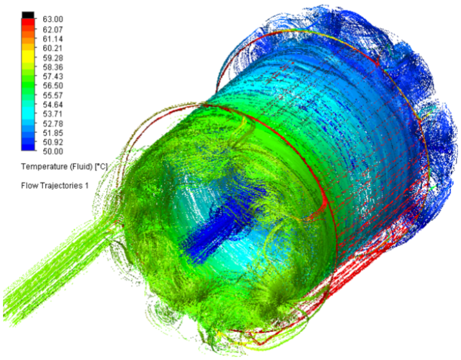

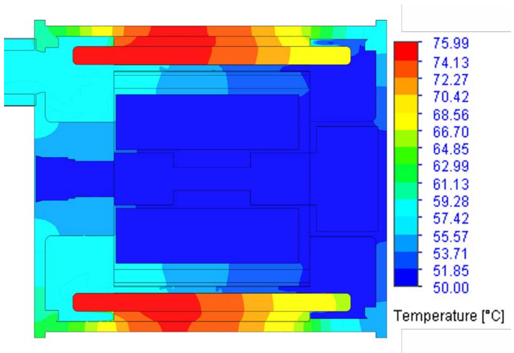

Figure 6.3 SolidWorks thermal & flow simulation Figure 6.4 SolidWorks – Simulated temperature distribution

7. CONCLUSION

In conclusion, this paper proposes an innovative design for an integrated Electro-Hydraulic Actuator (iEHA) by aggressively integrating the components of a linear hydraulic actuation system. The paper focuses on the design challenges of integrating the electric prime mover (EM), hydraulic pump, valve manifold, and Accumulator into a single-cylinder unit. Particular attention is given to key design areas. Such as the integration of the EM and the hydraulic pump (the E-pump), the concentric design approach for the cylinder and the Accumulator, and the utilization of differential flow to cool the E-pump.

Furthermore, the system's sizing is supported by two thermal simulation methods. A lumped-parameter model built in Siemens Amesim to verify the iEHA's design approach, with a particular focus on the E-pump's thermals. Additionally, a CFD simulation in Dassault Systèmes' SolidWorks confirmed the feasibility of the E-pump's cooling approach. These results demonstrate that the system temperature remains within acceptable limits and that the cooling architecture provides adequate flow to cool the E-pump evenly.

Though this paper focuses on simulation, the current work involves testing prototypes of the E-pump, the manifold, and the control system. In the future, the plan is to build a complete iEHA prototype based on lessons learned from both simulations and the prototyping phase. Once proven, the proposed iEHA concept could find wide application in several electrified areas, such as aerospace and electrified mobile machines, where efficiency is critical.

8. REFERENCES

[1] Huang, H., 2015, Challenges in More Electric Aircraft (MEA), IEEE Transportation Electrification, Community newsletter July/August 2015.

[2] Haack S., Flaig A., 2022, Sustainable Hydraulics for Industrial and Mobile Applications, 13th Int. Fluid Power Conference, Germany, June 2022. https://www.doi.org/10.18154/RWTH-2023-05258.

[3] D. Hagen, D. Padovani and M. Choux, "Guidelines to Select Between Self-Contained Electro-Hydraulic and Electromechanical Cylinders," *2020 15th IEEE Conference on Industrial Electronics and Applications (ICIEA)*, Kristiansand, Norway, 2020. https://www.doi.org/10.1109/ICIEA48937.2020.9248373.

[4] Vacca, Andrea, and Germano Franzoni. Hydraulic fluid power: Fundamentals, applications, and circuit design. John Wiley & Sons, 2021; ISBN: 978-1-119-56910-7.

[5] Li, Bo, Liu, Yongteng, Tan, Cao, Qin, Qijing and Lu, Yingtao. "Review on electro-hydrostatic actuator: System configurations, design methods and control technologies." International Journal of Mechatronics and Manufacturing Systems Vol. 13 No. 4 (2020): pp. 323–346. https://www.doi.org/10.1504/IJMMS.2020.112356

[6] Qu S., Fassbender D., Vacca A., Busquets E., 2021, A High-Efficient Solution for Electro-Hydraulic Actuators with Energy Regeneration Capability, Energy, Vol 2016, February 2021. https://www.doi.org/119291. 10.1016/j.energy.2020.119291.

[7] Shaoyang Qu, Federico Zappaterra, Andrea Vacca, Enrique Busquets, An electrified boom actuation system with energy regeneration capability driven by a novel electro-hydraulic unit, Energy Conversion and Management, Volume 293, 2023. https://www.doi.org/10.1016/j.enconman.2023.117443

[8] Qu, S., Zappaterra, F., Vacca, A., Liu, Z., & Busquets, E. (2023). Experimental Verification of An Electro-Hydraulic Actuation System Driven by An Integrated Electro-Hydraulic Unit. International Journal of Fluid Power. https://www.doi.org/10.13052/ijfp1439-9776.2427

[9] Pietrzyk, Tobias et al. "Design study of a high speed power unit for electro hydraulic actuators (EHA) in mobile applications." (2018). https://www.doi.org/10.18154/RWTH-2018-224632

[10] G. Altare, A. Vacca and C. Richter, "A novel pump design for an efficient and compact Electro-Hydraulic Actuator IEEE aerospace conference," 2014 IEEE Aerospace Conference, Big Sky, MT, USA, 2014. https://www.doi.org/10.1016/j.proeng.2015.06.003

[11] Rahmfeld, Robert, Monika Ivantysynova, and Jürgen Weber. "Displacement controlled wheel loader–a simple and clever solution." Proceedings of the 4th International Fluid Power Conference, Dresden, Germany. 2004.

[12] Federico Zappaterra, Andrea Vacca, Scott D. Sudhoff, A compact design for an

electric driven hydraulic gear machine capable of multiple quadrant operation, Mechanism and Machine Theory, Volume 177, 2022. https://www.doi.org/10.1016/j.mechmachtheory.2022.105024

[13] Federico Zappaterra, Dinghao Pan, Thomas Ransegnola, Andrea Vacca, Scott D. Sudhoff, Enrique Busquets, A novel electro-hydraulic unit design based on a shaftless integration of an internal gear machine and a permanent magnet electric machine, Energy Conversion and Management, Volume 310, 2024. https://doi.org/10.1016/j.enconman.2024.118432

[14] Andrea Vacca, Hassan Assaf, Hao Zhang, Federico Zappaterra, Integrated electrohydraulic actuator, 2023, Patent application: WO/2024/205693.

[15] Norrhydro, NorrDigi® EMA - Complete electromechanical solutions for superior energy-efficiency & reliable motion control, https://www.norrhydro.com/en/norrdigi_ema, Last accessed: 10/25/2025

[16] Ivantysyn, J. and Ivantysynova, M. 2001. Hydrostatic Pumps and Motors, Principles, Designs, Performance, Modelling, Analysis, Control and Testing. New Delhi. Academia Books International. ISBN 81-85522-16-2

[17] Hao Zhang, Federico Zappaterra, Satish Kumar Raju Kalidindi, Andrea Vacca, Hassan Assaf, Assemblies for an internal gear pump with hydrostatic support features, 2023, Patent application: WO/2024/205694.

[18] Andrea Vacca, Hassan Assaf, Satish Kumar Raju Kalidindi, Federico Zappaterra, Cooling configuration for an electric motor driving an electrohydraulic actuator, 2023, Patent application: WO/2024/205692.

[19] Ketelsen, S.; Padovani, D.; Andersen, T.O.; Ebbesen, M.K.; Schmidt, L. Classification and Review of Pump-Controlled Differential Cylinder Drives. Energies 2019. https://doi.org/10.3390/en12071293

[20] Shaoyang Qu, Federico Zappaterra, Andrea Vacca, Enrique Busquets, An electrified boom actuation system with energy regeneration capability driven by a novel electro-hydraulic unit, Energy Conversion and Management, Volume 293, 2023. https://doi.org/10.1016/j.enconman.2023.117443

[21] Sudhoff, Scott D. Power magnetic devices: a multi-objective design approach. John Wiley & Sons (2021). ISBN: 978-1-119-67463-4

Biographies

Seshan Calapatti Suresh received his bachelor's degree in Mechatronics Engineering from Acharya Institutes in 2019. He then pursued a master's degree in Mechatronics Engineering from Politecnico Di Torino, Italy. In 2022, he had the opportunity to complete his master's thesis at the Maha Fluid Power Research Centre (Maha), Purdue University, as a visiting scholar. This visiting scholarship led to my candidacy for a PhD at Maha.

Dr. Andrea Vacca is the director of the Maha Fluid Power Research Centre, the largest academic centre dedicated to fluid power and motion control research in the U.S. His research focuses on components and systems design to promote electrification, low noise emissions, high productivity, and concepts and techniques for condition monitoring. Andrea Vacca is the editor in chief for the International Journal of Fluid Power, a fellow of the American Society of Mechanical Engineers, and a director of the Global Fluid Power Society. In 2019, he also received the J. Bramah medal from the Institution of Mechanical Engineers. In 2025, he was inducted into the Fluid Power Hall of Fame by the International Fluid Power Society.

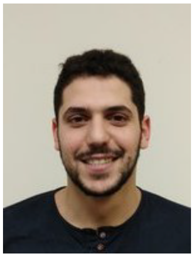

Dr. Hassan is Control Systems Senior Engineer at Caterpillar Inc. He specializes in development and tuning of electro-hydraulic systems and components. He completed his PhD at Purdue University in 2023 through the Maha Fluid Power Research Center. His doctoral research focused on developing Innovative Methods for Electro-Hydraulic Actuation and Fluid Power Education.

Dr. Zhang is a chief engineer and Parker Engineering Fellow at Parker Motion Systems Group, with over 20 years of experience in the motion control industry. He has led multiple market-driven technology roadmap establishments and directed the execution of technology development for mobile and industrial applications. He has led and coordinated internal and external resources in various advanced mobile electro-hydraulic components/systems development and commercialization activities. His current focus is on intelligent mobile hydraulic system controls with power-dense and efficient E-Pumps.